



## SOLAR WIND DECELERATION AT MARS AND EARTH: A COMPARISON

T. L. Zhang,\* K. Schwingenschuh,\* W. Riedler,\* G. Kotova,\*\*  
M. Verigin,\*\* M. Tatralayay\*\*\* and C. T. Russell†

\* *Space Research Institute, Graz, Austria*

\*\* *IKI, Moscow, Russia*

\*\*\* *KFKI, Budapest, Hungary*

† *IGPP, UCLA, U.S.A.*

### ABSTRACT

Phobos 2 plasma measurements have revealed the solar wind deceleration upstream of the Martian terminator bow shock. Earlier studies have shown that the solar wind is decelerated and deflected in the Earth's foreshock region. At Mars, the solar wind decelerated more at duskside than at dawnside. At Earth the solar wind decelerates most upstream of the quasi-parallel bow shock in the foreshock region. In this paper, we investigate and compare the solar wind deceleration at Mars and Earth.

© 1997 COSPAR. Published by Elsevier Science Ltd.

### INTRODUCTION

The deceleration of the solar wind is observed in the Earth's foreshock region [Bame et al., 1980; Bonifazi et al., 1980; Bonifazi et al., 1983; Formisano and Amata, 1976]. This deceleration is of an average of 7-10 km/s and it is correlated with the 'diffuse' but not with the 'reflected' ion population [Bame et al., 1980]. It has been suggested that the solar wind deceleration is a result of momentum transfer between the backstreaming ions and the solar wind ions through wave-particle interaction. Associated with this deceleration of speed, the direction of the solar wind is deflected slightly by around  $1^\circ$ .

Although the foreshock covers a large space in front of the bow shock, the solar wind deceleration at Earth occurs in certain part of the foreshock only. Zhang et al. [1995] examined the deceleration of solar wind at Earth and determined how this deceleration varies in the foreshock region. They find that the solar wind speed decreases most in front of the quasi-parallel bow shock. Along the IMF direction, this deceleration is seen to be a maximum near the bow shock and stops when the distance from bow shock reaches  $5 R_E$ .

Phobos 2 plasma measurements have revealed the solar wind deceleration upstream of the Martian terminator bow shock [Verigin et al., 1991; Kotova et al., 1996; Barabash and Lundin, 1993; Dubinin et al., 1994]. The solar wind deceleration is observed in all three elliptical orbits and in most of the circular orbits. This deceleration has been attributed to the mass loading by the ions originating from the hot oxygen/hydrogen corona of Mars and protons specularly reflected from the bow shock.

In this study, we investigate and compare the solar wind deceleration at Mars and Earth. At Earth, the solar wind speed decreases only in front of the quasi-parallel bow shock. At Mars, the solar wind deceleration is a common feature upstream of the Martian bow shock, for either quasi-parallel or quasi-perpendicular shocks. At both Earth and Mars, along the IMF direction, the solar wind deceleration is seen to be a maximum near the bow shock and decreases with the distance from the bow shock.

### OBSERVATIONS

Figure 1 presents the solar wind velocity measured by TAUS spectrometer during the first three elliptical orbits. Here we show the data one hour upstream of the bow shock crossing for the first three elliptical orbits. The solar

wind decelerates about 100 km/s upstream of the bow shock [Verigin *et al.*, 1991]. Of these three orbits, only the third orbit measurements are obtained when the spacecraft was three-axis stabilized. Thus we select the third orbit for our analysis.

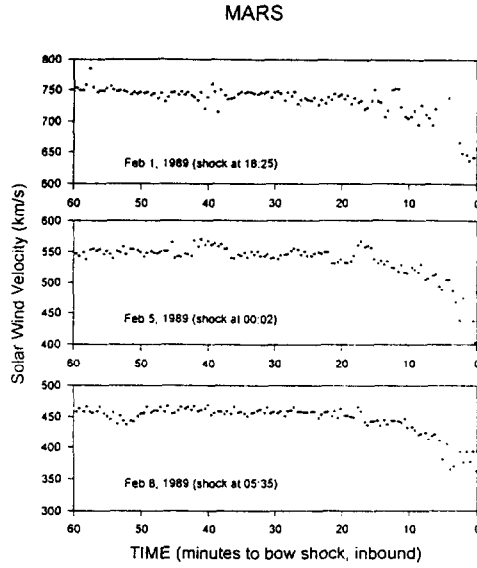


Figure 1. Solar wind velocity measured by TAUS spectrometer during the first three elliptical orbits.

Figure 2 shows the time series of plasma and magnetic field parameters one hour upstream of the bow shock from 0435 UT to 0535 UT, February 8, 1989. From the top: (a) Solar wind velocity measured by TAUS spectrometer. (b) The distance from spacecraft to bow shock along the IMF. Here we used the Martian bow shock model described by Zhang *et al.* [1991]. (c)  $\theta_{BN}$ , the angle between the normal of the model bow shock surface [Zhang *et al.*, 1991] and the magnetic field line at the point of crossing. (d)  $\sigma_c / \langle B \rangle$ , the normalized compressional components of the magnetic field fluctuations. (e)  $\sigma_t / \langle B \rangle$ , the normalized transverse components of the magnetic field fluctuations. The magnetic field fluctuations have been obtained by calculating the 30 sec standard deviations of 1.5 sec resolution magnetometer data:

$$\sigma_c = \left[ \frac{1}{N} \sum_{i=1}^N (|B|_i - |\bar{B}|)^2 \right]^{1/2}$$

$$\sigma_t = (\sigma_x^2 + \sigma_y^2 + \sigma_z^2 - \sigma_c^2)^{1/2}$$

where

$$\sigma_x^2 = \frac{1}{N} \sum_{i=1}^N (B_{xi} - \bar{B}_x)^2$$

$$\sigma_y^2 = \frac{1}{N} \sum_{i=1}^N (B_{yi} - \bar{B}_y)^2$$

$$\sigma_z^2 = \frac{1}{N} \sum_{i=1}^N (B_{zi} - \bar{B}_z)^2$$

In Figure 3 we present the solar wind deceleration example at Earth. The solar wind velocity was measured by the LASL/MPI crossed-fan solar wind ion experiment during 0600-1600 UT, December 1, 1977. Similar as in Figure 2, we performed the same analysis for the solar wind deceleration at Earth. In this study, we use the bow shock model of Fairfield [1971]. Here we calculate the  $\sigma_c / \langle B \rangle$  and  $\sigma_t / \langle B \rangle$  by 1 minute averages of the standard deviations of 4 sec resolution ISEE 1 magnetometer data.

Comparing Figure 2 and Figure 3, we find that both at Mars and Earth, the solar wind deceleration is seen to be a maximum near the bow shock and decreases with the distance from the bow shock. The solar wind deceleration upstream of the Mars and Earth bow shock varies in accord with the amplitude of the magnetic fluctuations. However, at Earth, the solar wind speed decreases only in front of the quasi-parallel bow shock. At Mars, the solar wind deceleration is a common feature upstream of the Martian bow shock, for either quasi-parallel or quasi-perpendicular shocks [Kotova et al., 1996]. To illustrate the  $\theta_{BN}$  dependence of the solar wind deceleration at Earth, we show in Figure 4 the solar wind deceleration as a function of  $\theta_{BN}$  [Zhang et al., 1995]. Solar wind deceleration starts around  $\theta_{BN}$  of  $50^\circ$  where the ULF foreshock starts [Le and Russell, 1992]. The solar wind decelerates most upstream of the quasi-parallel shock.

MARS

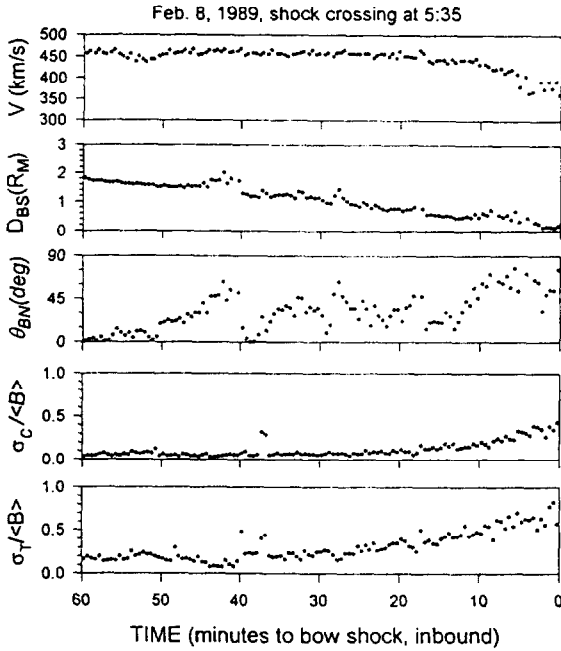


Figure 2. Sequence of the solar wind deceleration upstream of bow shock at Mars.

EARTH

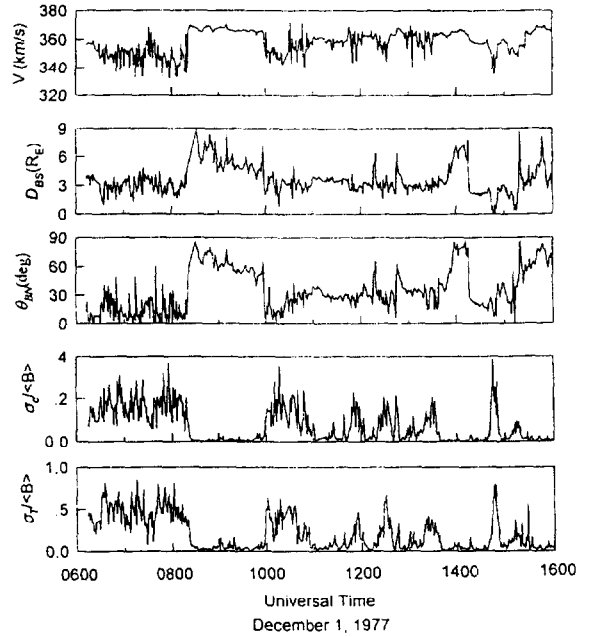


Figure 3. Sequence of the solar wind deceleration in the foreshock region at Earth.

EARTH

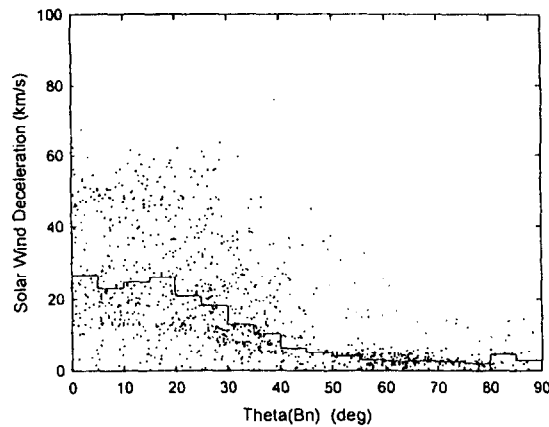


Figure 4. Solar wind deceleration at Earth's foreshock as a function of  $\theta_{BN}$  [Zhang et al, 1995]. The solid lines are the medians of the decelerations every  $5^\circ$  of  $\theta_{BN}$ .

## SUMMARY

At Earth, the solar wind speed decreases most in front of the quasi-parallel bow shock. This deceleration is caused by the so-called „diffuse“ ions backstreaming from the bow shock. At Mars, the solar wind deceleration is a common feature upstream of the Martian bow shock, for either quasi-parallel or quasi-perpendicular shocks [Kotova *et al.*, 1996]. The solar wind decelerated more at quasi-perpendicular shocks than at quasi-parallel shocks. Kotova *et al.* [1996] have suggested that this Mars solar wind deceleration is due to the mass loading by the ions originating from the hot oxygen/hydrogen corona of Mars and protons specularly reflected from the bow shock.

We find that both at Mars and Earth, the solar wind deceleration is seen to be a maximum near the bow shock and decreases with the distance from the bow shock. The solar wind deceleration upstream of the Mars and Earth bow shock varies in accord with the amplitude of the magnetic fluctuations.

## REFERENCES

- Bame, S. J., J. R. Asbridge, W. C. Feldman, J. T. Gosling, G. Paschmann and N. Sckopke, Deceleration of the solar wind upstream from the Earth's bow shock and the origin of diffuse upstream ions, *J. Geophys. Res.*, *85*, 2981, 1980.
- Barabash, S., and R. Lundin, Reflected ions near Mars: Phobos-2 observations, *Geophys. Res. Lett.*, *20*, 787-790, 1993.
- Bonifazi, C., G. Moreno, A. J. Lazarus and J. D. Sullivan, Deceleration of the solar wind in the Earth's foreshock region: Isee 2 and Imp 8 observations, *J. Geophys. Res.*, *85*, 6031, 1980.
- Bonifazi, C., G. Moreno, C. T. Russell, A. J. Lazarus and J. D. Sullivan, Solar wind deceleration and MHD turbulence in the Earth's foreshock region: ISEE 1 and 2 and IMP 8 observations, *J. Geophys. Res.*, *88*, 2029, 1983.
- Fairfield, D. H., Average and unusual locations of the Earth's magnetopause and bow shock, *J. Geophys. Res.*, *76*, 6700, 1971.
- Formisano, V., and E. Amata, Solar wind interaction with the Earth's magnetic field 4. Preshock perturbation of the solar wind, *J. Geophys. Res.*, *81*, 3907, 1976.
- Kotova, G., M. Verigin, A. Remizov, N. Shutte, H. Rosenbauer, S. Livi, K. Szegö, M. Tatrallyay, J. Slavin, J. Lemaire, K. Schwingenschuh, and T. L. Zhang, The study of the solar wind deceleration upstream of the Martian terminator bow shock, *J. Geophys. Res.*, *in press*, 1996.
- Le, G., and C. T. Russell, A study of ULF wave foreshock morphology-1: ULF foreshock boundary, *Planet. Space Sci.*, *40*, 1203, 1992.
- Dubinin, E., D. Obod, A. Pedersen, and R. Grard, Mass-loading asymmetry in the upstream region near Mars, *Geophys. Res. Lett.*, *21*, 2769-2772, 1994.
- Verigin, M. I., K. I. Gringauz, G. A. Kotova, N. M. Shutte, H. Rosenbauer, S. Livi, A. K. Richter, W. Riedler, K. Schwingenschuh and K. Szegö, On the problem of the Martian atmosphere dissipation: Phobos 2 TAUS spectrometer results, *J. Geophys. Res.*, *96*, 19315-19320, 1991.
- Zhang, T. L., K. Schwingenschuh, and C. T. Russell, A study of the solar wind deceleration in the Earth's foreshock region, *Adv. Space Res.*, *Vol. 15, No. 8/9*, 137-140, 1995.
- Zhang, T. L., K. Schwingenschuh, H. Lichtenegger, W. Riedler, C. T. Russell, and J. G. Luhmann, Interplanetary magnetic field control of the Mars bow shock: Evidence for Venus-like interaction, *J. Geophys. Res.*, *96*, 11265-11269, 1991.